The Hard Hexagon Partition Function for Complex Fugacity

Iwan Jensen

MASCOS,
Department of Mathematics and Statistics,
The University of Melbourne

ANZAMP Annual Meeting, Mooloolaba, November 27, 2013

Work with: M Assis, JL Jacobsen, J-M Maillard and BM McCoy

J. Phys. A **46**, 445202 (2013); arXiv: 1306.6389

Supported by the Australian Research Council.
Computing power provided by NCINF.

Hard Hexagons

The hard hexagon model is defined on a triangular lattice.

Hard Hexagons

The hard hexagon model is defined on a triangular lattice.

Particles are placed on the sites of the lattice with the restriction that particles are not allowed to occupy nearest neighbor sites.

Hard Hexagons

The hard hexagon model is defined on a triangular lattice.

Particles are placed on the sites of the lattice with the restriction that particles are not allowed to occupy nearest neighbor sites.

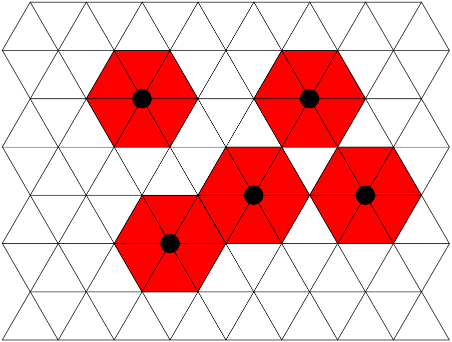

Baxter's solution for real z

Baxter computed the fugacity z and the partition function per site

$$\kappa_\pm(z) = \lim_{L_h \to \infty} \lambda_{\max}(z; L_h)^{1/L_h}$$

for positive z terms of an auxiliary variable x using the functions

$$\begin{aligned}
G(x) &= \prod_{n=1}^{\infty} \frac{1}{(1 - x^{5n-4})(1 - x^{5n-1})}, \\
H(x) &= \prod_{n=1}^{\infty} \frac{1}{(1 - x^{5n-3})(1 - x^{5n-2})}, \\
Q(x) &= \prod_{n=1}^{\infty} (1 - x^n).
\end{aligned}$$

Baxter's solution for real z

Baxter computed the fugacity z and the partition function per site

$$\kappa_\pm(z) = \lim_{L_h\to\infty} \lambda_{\max}(z; L_h)^{1/L_h}$$

for positive z terms of an auxiliary variable x using the functions

$$\begin{aligned}
G(x) &= \prod_{n=1}^{\infty} \frac{1}{(1-x^{5n-4})(1-x^{5n-1})}, \\
H(x) &= \prod_{n=1}^{\infty} \frac{1}{(1-x^{5n-3})(1-x^{5n-2})}, \\
Q(x) &= \prod_{n=1}^{\infty} (1-x^n).
\end{aligned}$$

Regions $0 \le z \le z_c \le z < \infty$ with $z_c = (11+5\sqrt{5})/2 = 11.090168\cdots$

Partition functions per site

For high density where $0 < z^{-1} < z_c^{-1}$ the results are

$$z = \frac{1}{x}\left(\frac{G(x)}{H(x)}\right)^5; \quad \kappa_+ = \frac{1}{x^{1/3}}\frac{G^3(x)\,Q^2(x^5)}{H^2(x)}\prod_{n=1}^{\infty}\frac{(1-x^{3n-2})(1-x^{3n-1})}{(1-x^{3n})^2}.$$

Partition functions per site

For high density where $0 < z^{-1} < z_c^{-1}$ the results are

$$z = \frac{1}{x}\left(\frac{G(x)}{H(x)}\right)^5; \quad \kappa_+ = \frac{1}{x^{1/3}}\frac{G^3(x)\,Q^2(x^5)}{H^2(x)}\prod_{n=1}^{\infty}\frac{(1-x^{3n-2})(1-x^{3n-1})}{(1-x^{3n})^2}.$$

As x increases from 0 to 1 the value of z^{-1} increases from 0 to z_c^{-1}.

Partition functions per site

For high density where $0 < z^{-1} < z_c^{-1}$ the results are

$$z = \frac{1}{x}\left(\frac{G(x)}{H(x)}\right)^5; \quad \kappa_+ = \frac{1}{x^{1/3}} \frac{G^3(x)\, Q^2(x^5)}{H^2(x)} \prod_{n=1}^{\infty} \frac{(1-x^{3n-2})(1-x^{3n-1})}{(1-x^{3n})^2}.$$

As x increases from 0 to 1 the value of z^{-1} increases from 0 to z_c^{-1}.

For low density where $0 \le z < z_c$

$$z = -x\left(\frac{H(x)}{G(x)}\right)^5; \quad \kappa_- = \frac{H^3(x)\, Q^2(x^5)}{G^2(x)} \prod_{n=1}^{\infty} \frac{(1-x^{6n-4})(1-x^{6n-3})^2(1-x^{6n-2})}{(1-x^{6n-5})(1-x^{6n-1})(1-x^{6n})^2}.$$

Partition functions per site

For high density where $0 < z^{-1} < z_c^{-1}$ the results are

$$z = \frac{1}{x}\left(\frac{G(x)}{H(x)}\right)^5; \quad \kappa_+ = \frac{1}{x^{1/3}} \frac{G^3(x)\,Q^2(x^5)}{H^2(x)} \prod_{n=1}^{\infty} \frac{(1-x^{3n-2})(1-x^{3n-1})}{(1-x^{3n})^2}.$$

As x increases from 0 to 1 the value of z^{-1} increases from 0 to z_c^{-1}.

For low density where $0 \leq z < z_c$

$$z = -x\left(\frac{H(x)}{G(x)}\right)^5; \quad \kappa_- = \frac{H^3(x)\,Q^2(x^5)}{G^2(x)} \prod_{n=1}^{\infty} \frac{(1-x^{6n-4})(1-x^{6n-3})^2(1-x^{6n-2})}{(1-x^{6n-5})(1-x^{6n-1})(1-x^{6n})^2}.$$

As x decreases from 0 to -1, the value of z increases from 0 to z_c.

Partition functions per site

For high density where $0 < z^{-1} < z_c^{-1}$ the results are

$$z = \frac{1}{x}\left(\frac{G(x)}{H(x)}\right)^5; \quad \kappa_+ = \frac{1}{x^{1/3}}\frac{G^3(x)\,Q^2(x^5)}{H^2(x)}\prod_{n=1}^{\infty}\frac{(1-x^{3n-2})(1-x^{3n-1})}{(1-x^{3n})^2}.$$

As x increases from 0 to 1 the value of z^{-1} increases from 0 to z_c^{-1}.

For low density where $0 \le z < z_c$

$$z = -x\left(\frac{H(x)}{G(x)}\right)^5; \quad \kappa_- = \frac{H^3(x)\,Q^2(x^5)}{G^2(x)}\prod_{n=1}^{\infty}\frac{(1-x^{6n-4})(1-x^{6n-3})^2(1-x^{6n-2})}{(1-x^{6n-5})(1-x^{6n-1})(1-x^{6n})^2}.$$

As x decreases from 0 to -1, the value of z increases from 0 to z_c.

$\kappa_\pm(z)$ have singularities at z_c, $z_d = -1/z_c$ and ∞.

The equimodular curve $|\kappa_-(z)| = |\kappa_+(z)|$

If the two eigenvalues $\kappa_-(z)$ and $\kappa_+(z)$ suffice to describe the partition function in the entire complex z plane then there will be zeros on the equimodular curve $|\kappa_-(z)| = |\kappa_+(z)|$.

The equimodular curve $|\kappa_-(z)| = |\kappa_+(z)|$

If the two eigenvalues $\kappa_-(z)$ and $\kappa_+(z)$ suffice to describe the partition function in the entire complex z plane then there will be zeros on the equimodular curve $|\kappa_-(z)| = |\kappa_+(z)|$. We numerically computed the curve from the parametric expressions of Baxter.

The equimodular curve $|\kappa_-(z)| = |\kappa_+(z)|$

If the two eigenvalues $\kappa_-(z)$ and $\kappa_+(z)$ suffice to describe the partition function in the entire complex z plane then there will be zeros on the equimodular curve $|\kappa_-(z)| = |\kappa_+(z)|$. We numerically computed the curve from the parametric expressions of Baxter.

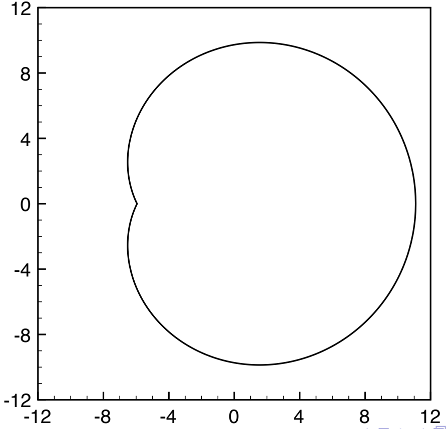

Partition functions zeros

The partition function on a lattice with L_v rows and L_h columns is

$$Z_{L_v,L_h}(z) \;=\; \sum g(N)\, z^N,$$

where $g(N)$ is the number of allowed configurations with N particles.

Partition functions zeros

The partition function on a lattice with L_v rows and L_h columns is

$$Z_{L_v,L_h}(z) = \sum g(N)\, z^N,$$

where $g(N)$ is the number of allowed configurations with N particles.

We use periodic boundary conditions in the horizontal direction such that $L_h + 1 \equiv 1$ and free boundary conditions in the vertical direction.

Partition functions zeros

The partition function on a lattice with L_v rows and L_h columns is

$$Z_{L_v,L_h}(z) \;=\; \sum g(N)\, z^N,$$

where $g(N)$ is the number of allowed configurations with N particles.

We use periodic boundary conditions in the horizontal direction such that $L_h + 1 \equiv 1$ and free boundary conditions in the vertical direction.

We restricted our attention to $L_h/3$ integer valued, commensurate with hexagonal ordering in the high density phase.

Partition functions zeros

The partition function on a lattice with L_v rows and L_h columns is

$$Z_{L_v,L_h}(z) \;=\; \sum g(N)\, z^N,$$

where $g(N)$ is the number of allowed configurations with N particles.

We use periodic boundary conditions in the horizontal direction such that $L_h + 1 \equiv 1$ and free boundary conditions in the vertical direction.

We restricted our attention to $L_h/3$ integer valued, commensurate with hexagonal ordering in the high density phase.

By definition on a finite lattice the partition function is a polynomial which can be described by its zeros z_k as $\prod(1 - z/z_k)$.

Partition functions zeros

The partition function on a lattice with L_v rows and L_h columns is

$$Z_{L_v,L_h}(z) \;=\; \sum g(N)\, z^N,$$

where $g(N)$ is the number of allowed configurations with N particles.

We use periodic boundary conditions in the horizontal direction such that $L_h + 1 \equiv 1$ and free boundary conditions in the vertical direction.

We restricted our attention to $L_h/3$ integer valued, commensurate with hexagonal ordering in the high density phase.

By definition on a finite lattice the partition function is a polynomial which can be described by its zeros z_k as $\prod(1 - z/z_k)$.

Much qualitative and quantitative information can be gained from the distribution of these zeros.

Partition functions zeros

The partition function on a lattice with L_v rows and L_h columns is

$$Z_{L_v,L_h}(z) \;=\; \sum g(N)\, z^N,$$

where $g(N)$ is the number of allowed configurations with N particles.

We use periodic boundary conditions in the horizontal direction such that $L_h + 1 \equiv 1$ and free boundary conditions in the vertical direction.

We restricted our attention to $L_h/3$ integer valued, commensurate with hexagonal ordering in the high density phase.

By definition on a finite lattice the partition function is a polynomial which can be described by its zeros z_k as $\prod(1 - z/z_k)$.

Much qualitative and quantitative information can be gained from the distribution of these zeros.

Numerically we compute the partition function using a transfer matrix algorithm to build the finite lattice site-by-site.

Hard hexagon partition function zeros

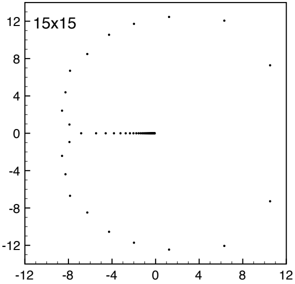

Hard hexagon partition function zeros

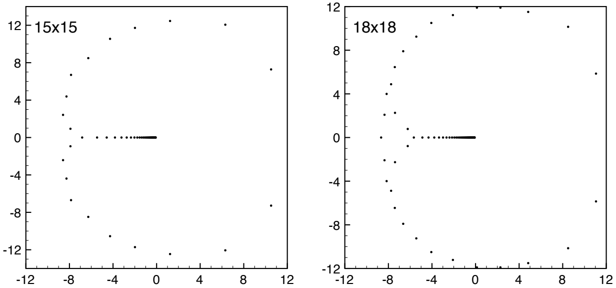

Hard hexagon partition function zeros

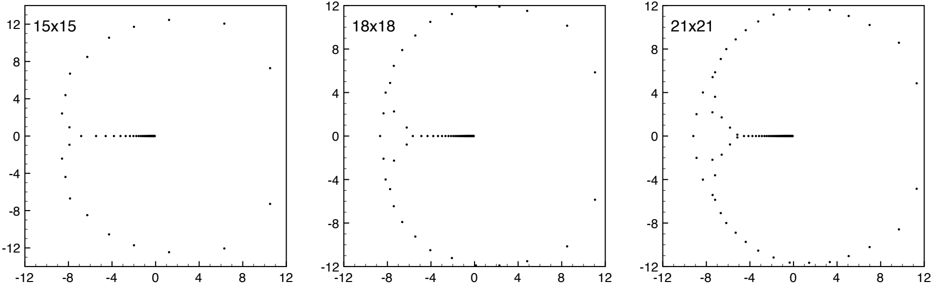

Hard hexagon partition function zeros

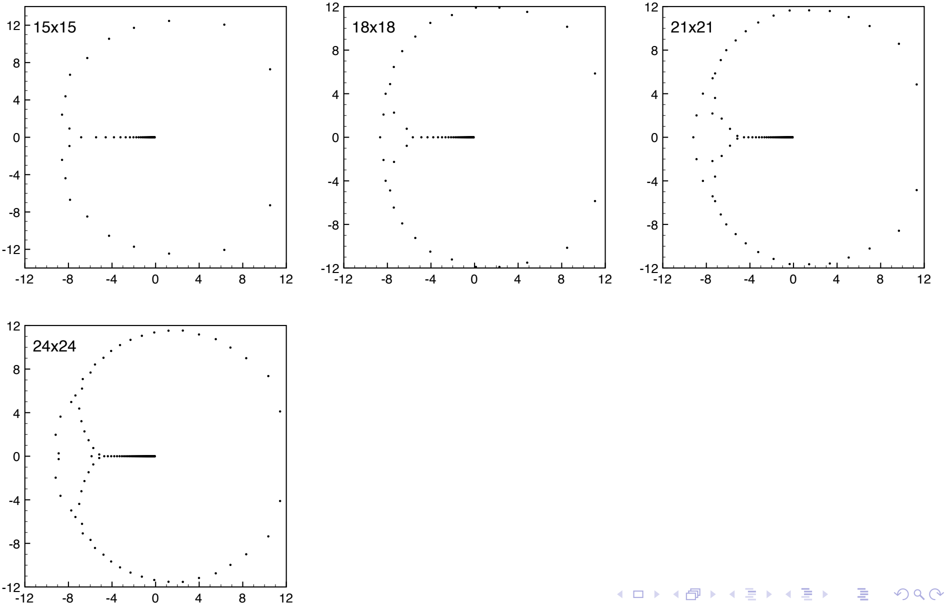

Hard hexagon partition function zeros

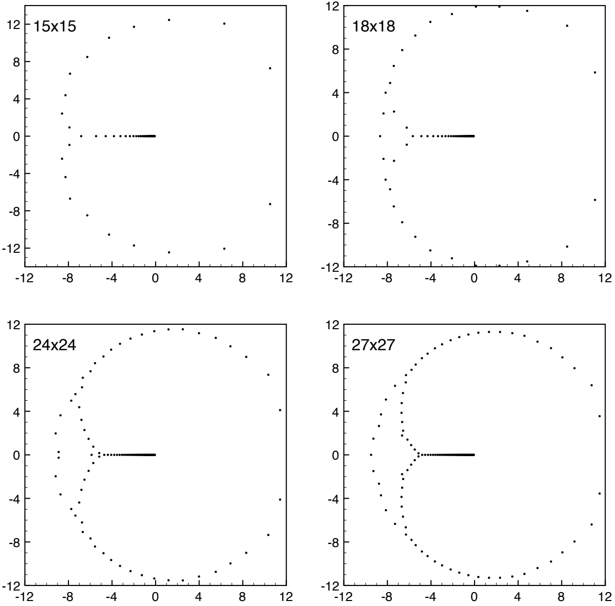

Hard hexagon partition function zeros

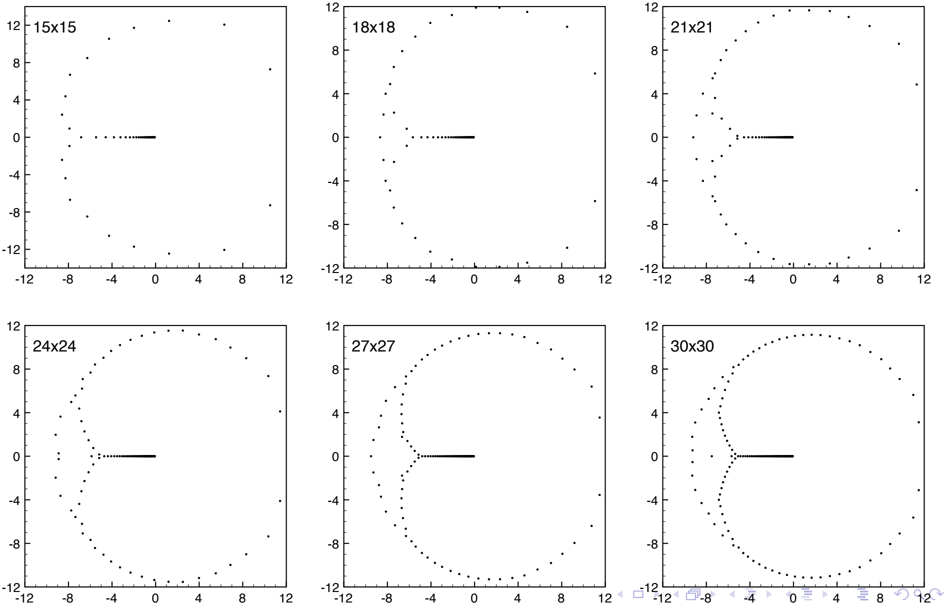

Hard hexagon partition function zeros

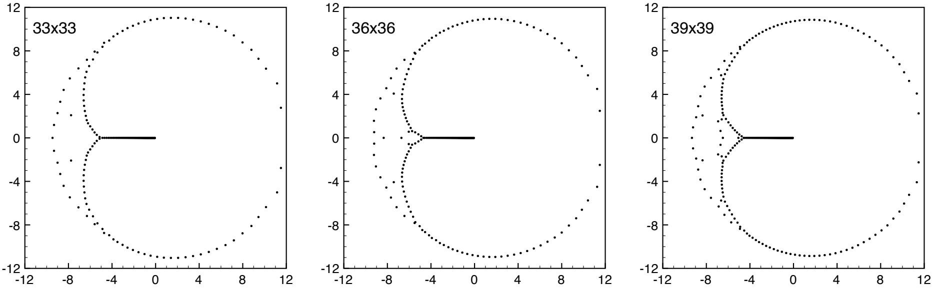

Hard hexagon partition function zeros

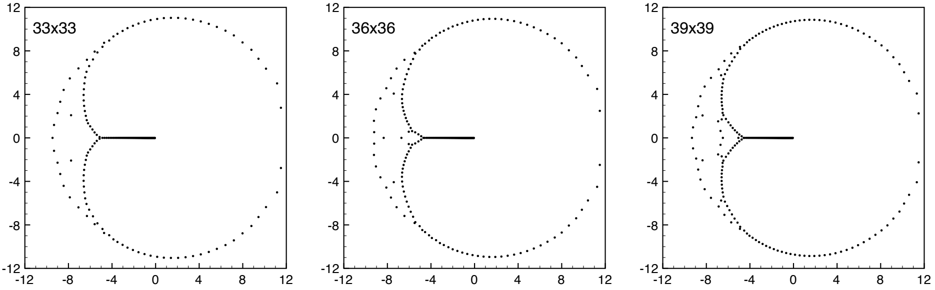

1. There is a 'necklace' on the left side. Baxter's solution does not tell the whole story.

Hard hexagon partition function zeros

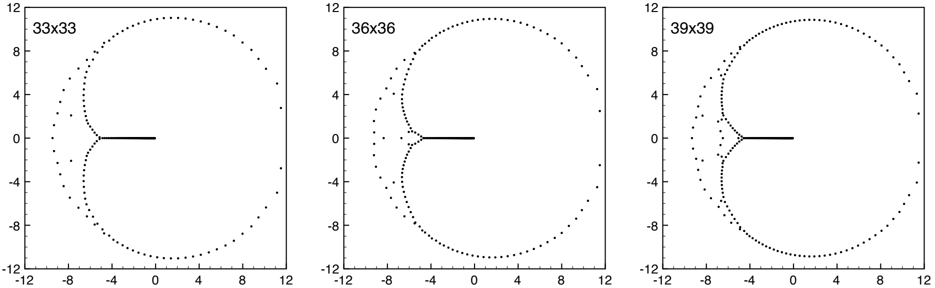

1. There is a 'necklace' on the left side. Baxter's solution does not tell the whole story.

2. Starting with 30 $\times$ 30 zeros start to appear in the necklace and separated regions begin to be apparent.

Hard hexagon partition function zeros

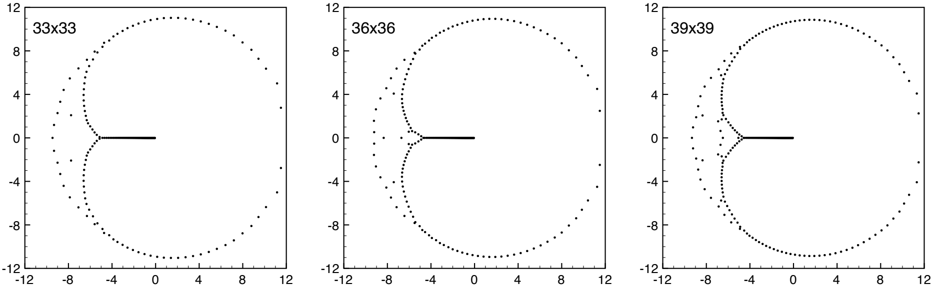

1. There is a 'necklace' on the left side. Baxter's solution does not tell the whole story.

2. Starting with 30×30 zeros start to appear in the necklace and separated regions begin to be apparent.

3. It is unknown what will happen as $L \to \infty$. Will the zeros fill the entire necklace region?

Hard hexagon partition function zeros

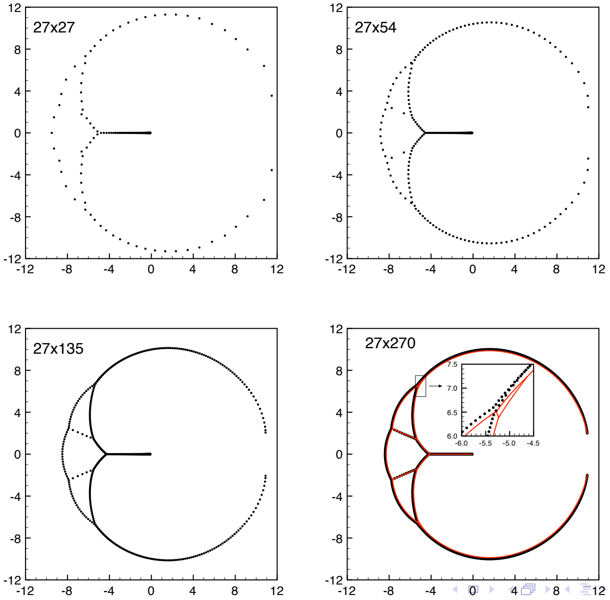

Transfer Matrix Eigenvalues

An alternative representation of the partition function on a finite lattice is given in terms of the eigenvalues of the transfer matrix $\mathbf{T}_{L_h}(z)$.

Transfer Matrix Eigenvalues

An alternative representation of the partition function on a finite lattice is given in terms of the eigenvalues of the transfer matrix $\mathbf{T}_{L_h}(z)$.

When the transfer matrix is diagonalizable the partition function may be written in terms of the eigenvalues λ_k and eigenvectors $\mathbf{v}_k$ of the transfer matrix

Transfer Matrix Eigenvalues

An alternative representation of the partition function on a finite lattice is given in terms of the eigenvalues of the transfer matrix $\mathbf{T}_{L_h}(z)$.

When the transfer matrix is diagonalizable the partition function may be written in terms of the eigenvalues λ_k and eigenvectors $\mathbf{v}_k$ of the transfer matrix $\mathbf{T}_{L_h}(z)$ as

$$Z_{L_v,L_h}(z) = \sum_k \lambda_k^{L_v}(z; L_h) c_k$$

where

$$c_k = (\mathbf{v_B} \cdot \mathbf{v_k})(\mathbf{v_k} \cdot \mathbf{v'_B}).$$

and $\mathbf{v_B}$ and $\mathbf{v'_B}$ are suitable vectors for the boundary conditions on rows 1 and L_v.

Zeros and Equimodular Curves

In the case where $L_v \to \infty$ with L_h fixed we are looking at infinite strips.

Zeros and Equimodular Curves

In the case where $L_v \to \infty$ with L_h fixed we are looking at infinite strips.

The zeros will accumulate on curves where the leading transfer matrix eigenvalues have equal modulus

$$|\lambda_1(z; L_h)| = |\lambda_2(z; L_h)|$$

Zeros and Equimodular Curves

In the case where $L_v \to \infty$ with L_h fixed we are looking at infinite strips.

The zeros will accumulate on curves where the leading transfer matrix eigenvalues have equal modulus

$$|\lambda_1(z; L_h)| = |\lambda_2(z; L_h)|$$

On this curve $\lambda_1(z; L_h)/\lambda_2(z; L_h) = e^{i\phi(z)}$ with $\phi(z)$ real.

Zeros and Equimodular Curves

In the case where $L_v \to \infty$ with L_h fixed we are looking at infinite strips.

The zeros will accumulate on curves where the leading transfer matrix eigenvalues have equal modulus

$$|\lambda_1(z; L_h)| = |\lambda_2(z; L_h)|$$

On this curve $\lambda_1(z; L_h)/\lambda_2(z; L_h) = e^{i\phi(z)}$ with $\phi(z)$ real.

The density of zeros on this curve is proportional to $d\phi(z)/dz$.

Calculating Equimodular Curves

We don't actually calculate the eigenvalues directly from $\mathbf{T}_{L_h}(z)$.

Calculating Equimodular Curves

We don't actually calculate the eigenvalues directly from $\mathbf{T}_{L_h}(z)$.

We use iterative diagonalisation methods where one studies not $\mathbf{T}$ itself but rather its repeated action on a suitable set of vectors.

Calculating Equimodular Curves

We don't actually calculate the eigenvalues directly from $\mathbf{T}_{L_h}(z)$.

We use iterative diagonalisation methods where one studies not $\mathbf{T}$ itself but rather its repeated action on a suitable set of vectors.

We work with vectors $\mathbf{T^n w}$ produced by the power method.

Calculating Equimodular Curves

We don't actually calculate the eigenvalues directly from $\mathbf{T}_{L_h}(z)$.

We use iterative diagonalisation methods where one studies not $\mathbf{T}$ itself but rather its repeated action on a suitable set of vectors.

We work with vectors $\mathbf{T^n w}$ produced by the power method.

An iterative scheme that works well even in the presence of complex and degenerate eigenvalues is known as Arnoldi's method.

Calculating Equimodular Curves

We don't actually calculate the eigenvalues directly from $\mathbf{T}_{L_h}(z)$.

We use iterative diagonalisation methods where one studies not $\mathbf{T}$ itself but rather its repeated action on a suitable set of vectors.

We work with vectors $\mathbf{T}^{\mathbf{n}}\mathbf{w}$ produced by the power method.

An iterative scheme that works well even in the presence of complex and degenerate eigenvalues is known as Arnoldi's method.

We make use of the public domain software package ARPACK implementing Arnoldi's method with suitable subtle stopping criteria.

Calculating Equimodular Curves

We don't actually calculate the eigenvalues directly from $\mathbf{T}_{L_h}(z)$.

We use iterative diagonalisation methods where one studies not $\mathbf{T}$ itself but rather its repeated action on a suitable set of vectors.

We work with vectors $\mathbf{T^n w}$ produced by the power method.

An iterative scheme that works well even in the presence of complex and degenerate eigenvalues is known as Arnoldi's method.

We make use of the public domain software package ARPACK implementing Arnoldi's method with suitable subtle stopping criteria.

The ARPACK package allows one to calculate eigenvalues (and eigenvectors) based on various criteria, including the one relevant to our calculations, namely the eigenvalues of largest modulus.

Calculating Equimodular Curves

We don't actually calculate the eigenvalues directly from $\mathbf{T}_{L_h}(z)$.

We use iterative diagonalisation methods where one studies not $\mathbf{T}$ itself but rather its repeated action on a suitable set of vectors.

We work with vectors $\mathbf{T^n w}$ produced by the power method.

An iterative scheme that works well even in the presence of complex and degenerate eigenvalues is known as Arnoldi's method.

We make use of the public domain software package ARPACK implementing Arnoldi's method with suitable subtle stopping criteria.

The ARPACK package allows one to calculate eigenvalues (and eigenvectors) based on various criteria, including the one relevant to our calculations, namely the eigenvalues of largest modulus.

We developed routines to automatically trace equimodular curves.

Hard hexagon equimodular curves

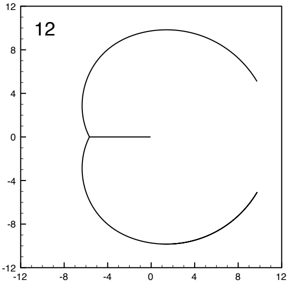

Hard hexagon equimodular curves

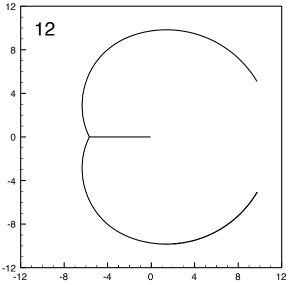

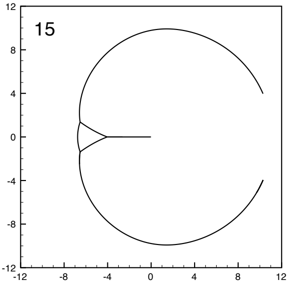

Hard hexagon equimodular curves

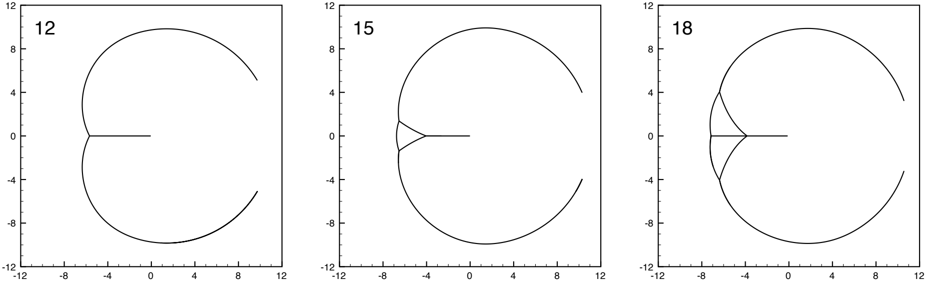

Hard hexagon equimodular curves

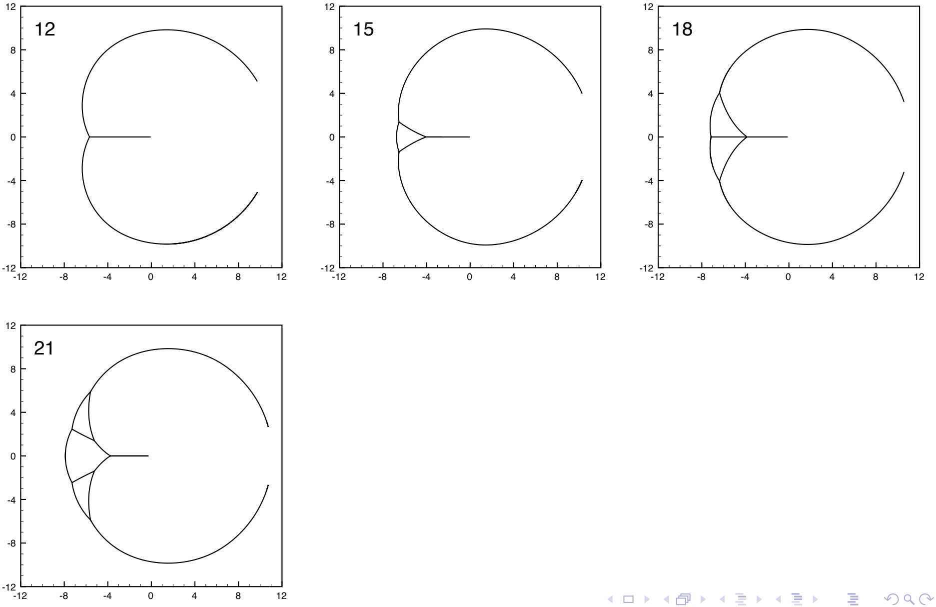

Hard hexagon equimodular curves

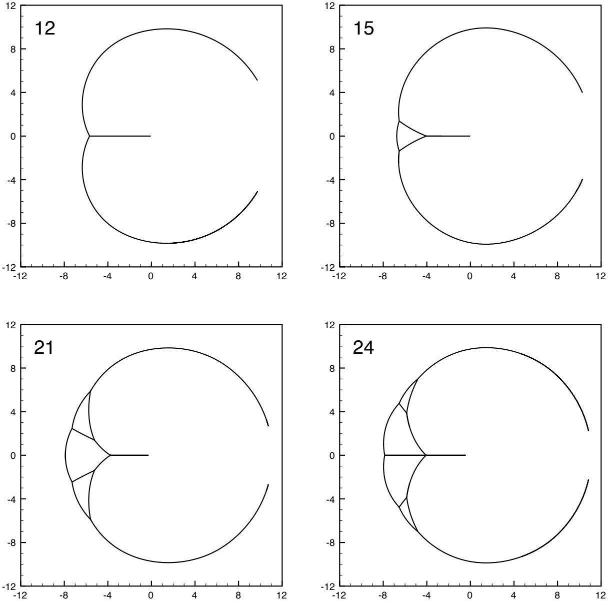

Hard hexagon equimodular curves

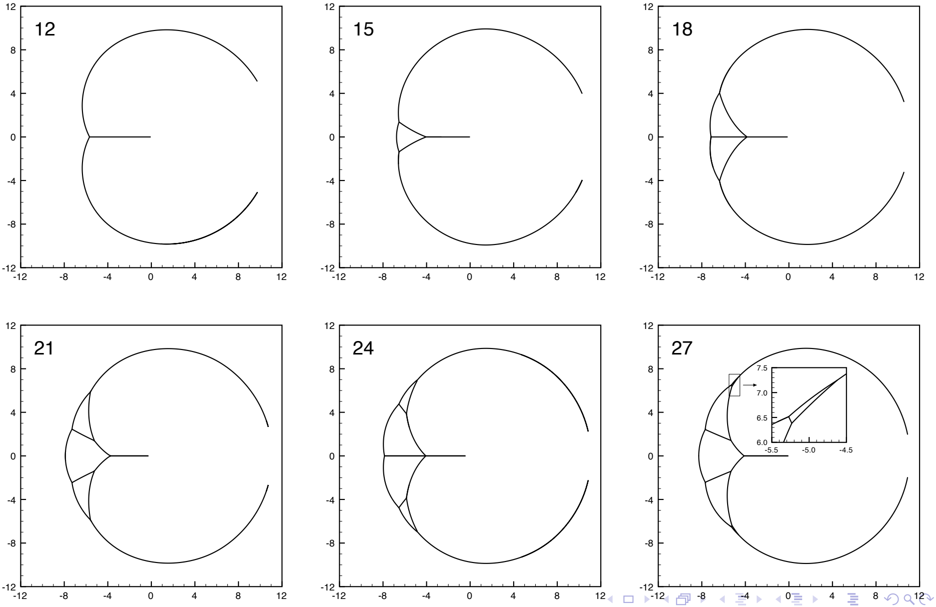

Hard hexagon equimodular curves

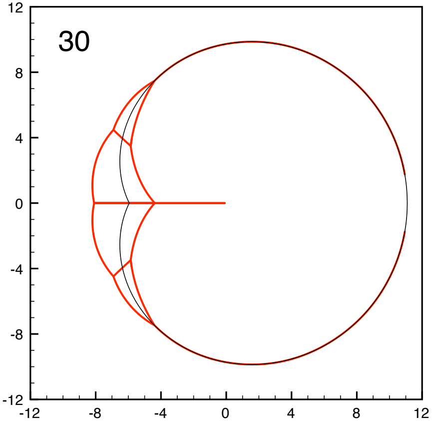

Dominant eigenvalue crossings in red; $|\kappa_-(z)| = |\kappa_+(z)|$ in black.

Just for fun. Some Hard Squares results

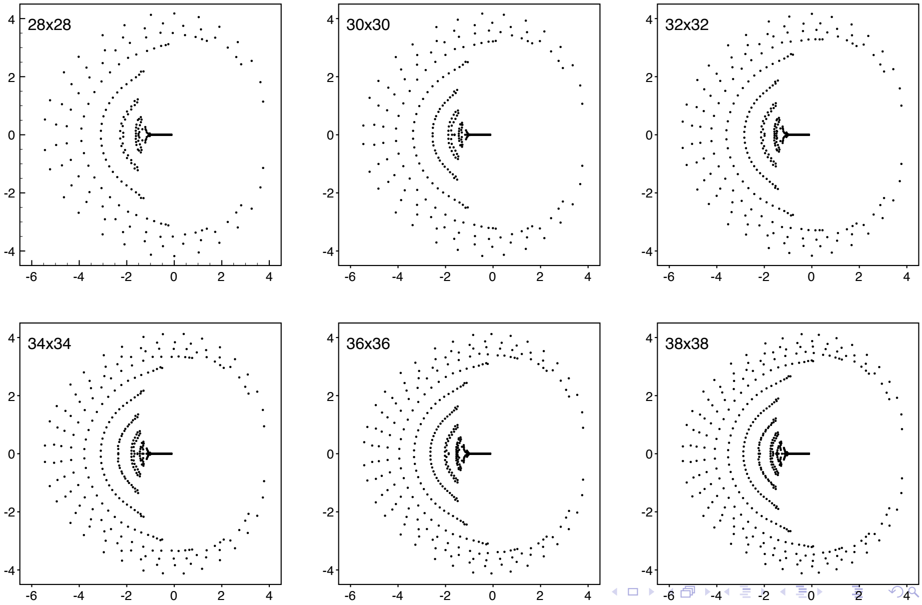

Just for fun. Some Hard Squares results

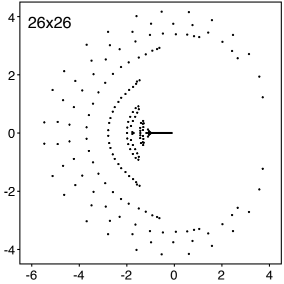

Just for fun. Some Hard Squares results

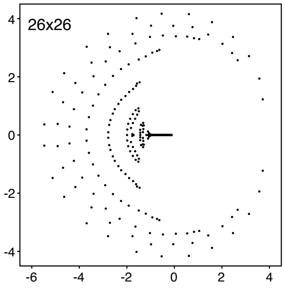

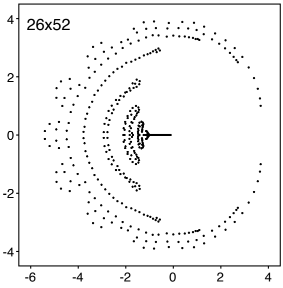

Just for fun. Some Hard Squares results

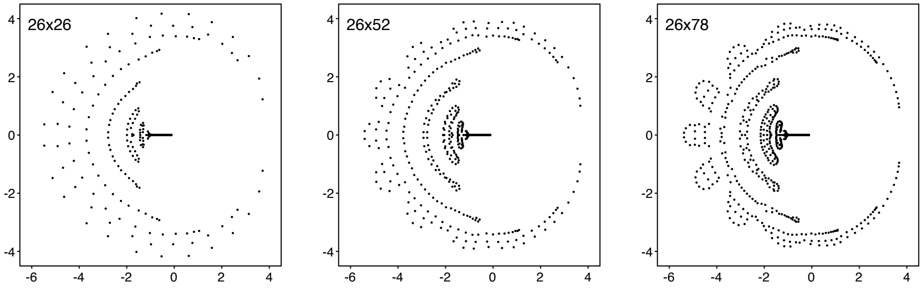

Just for fun. Some Hard Squares results

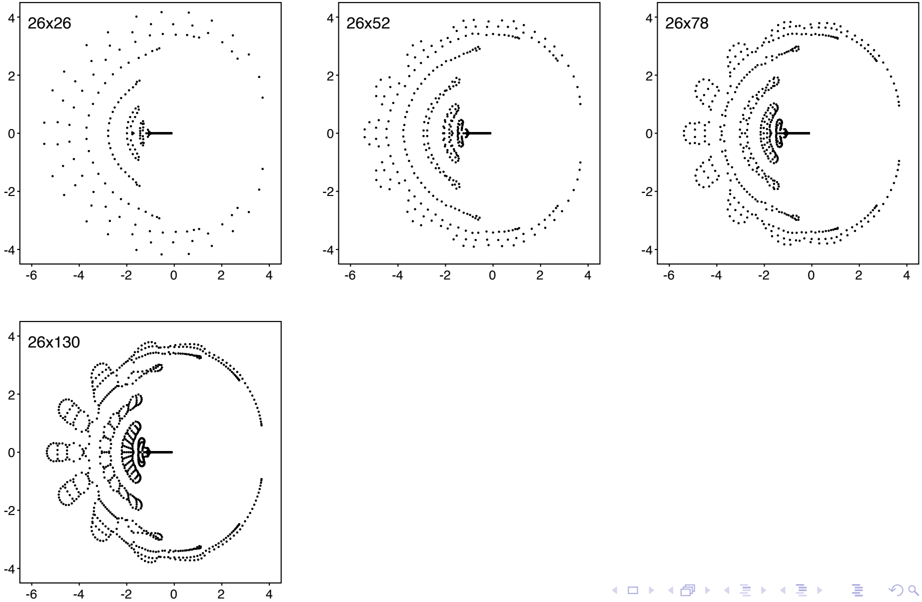

Just for fun. Some Hard Squares results

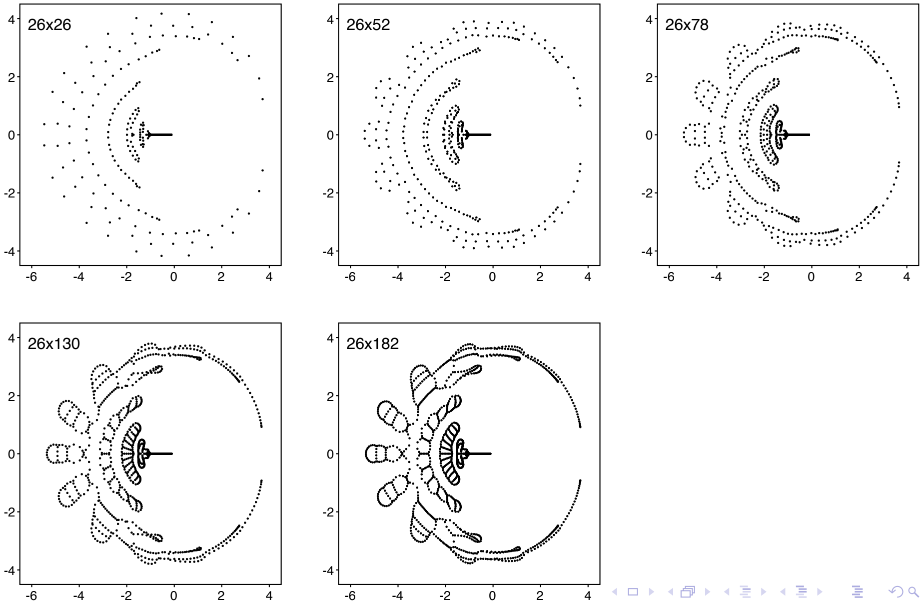

Just for fun. Some Hard Squares results

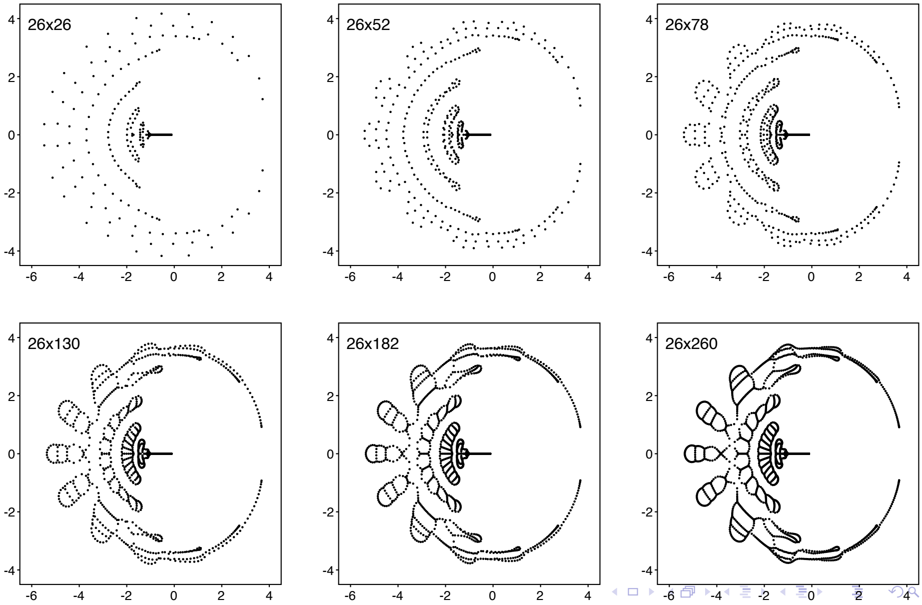

It's not just about pretty pictures

According to finite-size scaling the free energy per site corresponding to the j-th eigenvalue of the transfer matrix has the scaling form

$$\frac{1}{L} f_j \left(|z - z_c| L^y, uL^{-|y'|} \right) ,$$

where z_c is the critical point, y is the leading relevant eigenvalue and u is the coupling to an irrelevant operator with eigenvalue $y' < 0$, which implies at leading order that

$$|z - z_c| = AL^{-y} + BuL^{-y-|y'|} + \dots ,$$

where A and B are non-universal constants.

It's not just about pretty pictures

According to finite-size scaling the free energy per site corresponding to the j-th eigenvalue of the transfer matrix has the scaling form

$$\frac{1}{L} f_j \left(|z - z_c| L^y, u L^{-|y'|} \right) ,$$

where z_c is the critical point, y is the leading relevant eigenvalue and u is the coupling to an irrelevant operator with eigenvalue $y' < 0$, which implies at leading order that

$$|z - z_c| = A L^{-y} + B u L^{-y-|y'|} + \dots ,$$

where A and B are non-universal constants.

To higher orders, terms on the RHS involve powers of L^{-1} that can be any non-zero linear combination of y and $|y'|$ with non-negative integer coefficients.

Finite-size behaviour at z_c

The critical point $z_c > 0$ of hard hexagons is known to be in the same universality class as the three-state ferromagnetic Potts model.

Finite-size behaviour at z_c

The critical point $z_c > 0$ of hard hexagons is known to be in the same universality class as the three-state ferromagnetic Potts model.

This provides the dominant eigenvalue $y = 6/5$ with subdominant eigenvalues $y' = -4/5$ and $y'' = -4$ respectively.

Finite-size behaviour at z_c

The critical point $z_c > 0$ of hard hexagons is known to be in the same universality class as the three-state ferromagnetic Potts model.

This provides the dominant eigenvalue $y = 6/5$ with subdominant eigenvalues $y' = -4/5$ and $y'' = -4$ respectively.

Our numerical analysis of $|z_c(L)| - z_c$ for L up to 39 gives good evidence for the scaling form

$$|z_c(L)| - z_c = a_0 L^{-6/5} + a_1 L^{-2} + a_2 L^{-14/5} + \dots$$

Finite-size behaviour at z_c

The critical point $z_c > 0$ of hard hexagons is known to be in the same universality class as the three-state ferromagnetic Potts model.

This provides the dominant eigenvalue $y = 6/5$ with subdominant eigenvalues $y' = -4/5$ and $y'' = -4$ respectively.

Our numerical analysis of $|z_c(L)| - z_c$ for L up to 39 gives good evidence for the scaling form

$$|z_c(L)| - z_c = a_0 L^{-6/5} + a_1 L^{-2} + a_2 L^{-14/5} + \ldots$$

The powers of L^{-1} appearing on the right-hand side can be identified with y, $y + |y'|$ and $y + 2|y'|$.

Finite-size behaviour at z_c

The critical point $z_c > 0$ of hard hexagons is known to be in the same universality class as the three-state ferromagnetic Potts model.

This provides the dominant eigenvalue $y = 6/5$ with subdominant eigenvalues $y' = -4/5$ and $y'' = -4$ respectively.

Our numerical analysis of $|z_c(L)| - z_c$ for L up to 39 gives good evidence for the scaling form

$$|z_c(L)| - z_c = a_0 L^{-6/5} + a_1 L^{-2} + a_2 L^{-14/5} + \dots$$

The powers of L^{-1} appearing on the right-hand side can be identified with y, $y + |y'|$ and $y + 2|y'|$.

This is compatible with the above general result.

Finite-size behaviour at z_c

The critical point $z_c > 0$ of hard hexagons is known to be in the same universality class as the three-state ferromagnetic Potts model.

This provides the dominant eigenvalue $y = 6/5$ with subdominant eigenvalues $y' = -4/5$ and $y'' = -4$ respectively.

Our numerical analysis of $|z_c(L)| - z_c$ for L up to 39 gives good evidence for the scaling form

$$|z_c(L)| - z_c = a_0 L^{-6/5} + a_1 L^{-2} + a_2 L^{-14/5} + \ldots$$

The powers of L^{-1} appearing on the right-hand side can be identified with y, $y + |y'|$ and $y + 2|y'|$.

This is compatible with the above general result.

However, note that powers such as $y + 1 = 11/5$ and $2y = 12/5$, which are possible in principle, are not observed numerically.

Finite-size behaviour at z_d

The CFT of the Lee-Yang point $z_d < 0$ is much simpler. There is only one non-trivial primary operator leading to the eigenvalue $y = 12/5$.

Finite-size behaviour at z_d

The CFT of the Lee-Yang point $z_d < 0$ is much simpler. There is only one non-trivial primary operator leading to the eigenvalue $y = 12/5$.

Our numerical analysis of $|z_d(L) - z_d|$ gives strong evidence for the scaling form

$$|z_d(L) - z_d| = b_0 L^{-12/5} + b_1 L^{-17/5} + b_2 L^{-22/5} + \dots$$

The powers of L^{-1} on the right-hand side can be identified with y, $y + 1$ and $y + 2$.

Finite-size behaviour at z_d

The CFT of the Lee-Yang point $z_d < 0$ is much simpler. There is only one non-trivial primary operator leading to the eigenvalue $y = 12/5$.

Our numerical analysis of $|z_d(L) - z_d|$ gives strong evidence for the scaling form

$$|z_d(L) - z_d| = b_0 L^{-12/5} + b_1 L^{-17/5} + b_2 L^{-22/5} + \dots$$

The powers of L^{-1} on the right-hand side can be identified with y, $y + 1$ and $y + 2$.

The integer shifts can be related to descendent operators in the CFT, since $|y'|$ is a positive integer for descendents of the identity operator.